ISSN 1846-6168 (Print), ISSN 1848-5588 (Online)
https://doi.org/10.31803/tg-20240506194710

Preliminary communication
Received: 2024-05-06, Accepted: 2024-09-11

Enhancement of Powder Mixed Electrical Discharge Machining Performance Using Nano SiO_2 Powder Additive

Dunya Adnan Ghulam*, Abbas Fadhil Ibrahim

Abstract: Nanopowder-mixed EDM was employed to machine metals that are challenging to machine by traditional processes. In this study, Inconel 718 was machined by adding nano-SiO_2 to a soybean oil dielectric with the use of magnetic field to enhance the process's functioning. The impact of machining factors (current, pulse on time, SiO_2 concentration, and magnetic field) on white layer thickness (*WLT*), heat-affected zone (*HAZ*), surface roughness (*Ra*), material removal rate (*MRR*), tool wear rate (*TWR*), and surface crack density (*SCD*) were studied. The findings demonstrated that adding nano-SiO_2 to the insulating fluid improved process's functioning, whereas the *WLT* and *HAZ* were enhanced by 37.68% and 42.16%, respectively. Also, *Ra*, *MRR*, and *TWR* were improved by 9.59%, 50.93%, and 66.44%, respectively, as compared to machining without powder addition. The SEM micrographs revealed that fewer cracks were produced on the workpiece's surface with 4 g/l of added SiO_2, and the *SCD* improved by 12.81%.

Keywords: Inconel 718; magnetic field assistance; NPMEDM; nano SiO_2; white layer thickness

1 INTRODUCTION

Shear force is employed in processes of traditional machining to form the machined parts to the required shape. When dealing with processed materials that possess elevated toughness and hardness levels, these processes become challenging to complete. This is because of the wear caused by the friction and the deformation process between the machined part and the used tool. Therefore, non-traditional processes were used, which involve thermal processes such as electrical discharge machining (EDM), which is one of the most widely used machining techniques to machine hard to machine materials by conventional processes [1]. In (EDM), the electrical energy transforms into thermal energy, which develops a plasma channel between the electrode and the workpiece, which causes the surface of the workpiece to vaporize after melting. EDM is effective for machining intricate shapes of any conductive material, regardless of its properties because it is contactless process [2-4]. A series of pulses are applied in the EDM process to both of the electrodes, i.e., the tool and the workpiece, which are separated by a very tiny gap called the machining gap, in which the plasma channel develops [5]. However, the application of EDM is limited by some aspects, like poor surface finish, craters, holes, voids, and cracks [6]. To overcome these limitations, a powder mixed electrical discharge machining (PMEDM) technique is used, in which powders are combined with the insulating fluid to modify the machined surface [7]. The added fine powders with suitable concentrations lower the breakdown strength of the dielectric fluid, modify the plasma channel, enlarge the gap distance, and helps the sparking to be uniformly distributed in the machining zone, resulting in an enhancement of machining performance [8]. Nickel based alloys are difficult to machine by traditional methods because of their high toughness and strength; therefore, the PMEDM process is an efficient way to machine them.

Many researchers have studied the machining of Inconel alloys using this process by adding different powders to various dielectric fluids. Inconel 718 machining and improving the performance of NPMEDM process was studied by adding nano alumina powder and using copper tungsten electrode. As compared to traditional electrical discharge machining, MRR was enhanced by 50% when using Nano alumina powder added to kerosene [9]. To enhance the performance of EDM process in purview surface integrity, *TWR*, and *MRR*, a 0.5 g/l of multi walled carbon nano tubes (MWCNT) was added to kerosene to machine Inconel 718 by [10]. Findings detected that MRR was improved by 44.95 %. *TWR* and *SR* decreased by 64.1 % and 14.1 % respectively as compared to traditional EDM. The reduction in recast layer thickness was 16.28% when using 0.5 g/l of MWCNT. In [11] authors studied graphene nanofluid added to deionized water used as a dielectric fluid. The impact of Ton, V, and I on *SR*, *TWR* and *MRR* were investigated. It was concluded that *SR*, *TWR*, *MRR* enhanced by 14 %, 2 %, and 20.1 % respectively. A. Ranjan et al. investigated Inconel 718 machining by adding four kinds of powders (aluminum, aluminum oxide, silicon carbide, as well as graphite) to EDM oil. The obtained results showed that when powders were added, the *MRR* improved by 5.93%, while when surfactant was added, the *MRR* improved by 13.56 %. Also, the SR was lowered by 43.9 % when adding powders and by 45.05 % when adding surfactant. The best SF was obtained when Gr powder was used due to its low density [12]. Influence of adding different concentrations of Nano SiC to EDM oil was examined for machining Inconel 718 superalloy by [13]. The authors concluded that adding Nano silicon carbide at 0.4 g/l enhanced the MRR by 163 %, while *SR* and *TWR* were eliminated approximately by 17 % and 24 %, respectively. Also, the WLT was significantly lowered after the addition of Nano silicon carbide. The effect of adding Nano alumina to deionized water on *TWR*, *SR*, as well as *MRR* was examined by [14]. It was concluded that *MRR* was higher by about 7 % as compared to conventional EDM. As well as the *TWR* and *SR* were eliminated by 6 % and 10 %, respectively. S. Kumar investigated a hybrid method of EDM used to operate Inconel

706, adding silicon carbide and boron carbide powders with magnetic field assistance. The results showed that the maximum material removal rate produced using the B_4C powder with the highest level of magnetic field intensity 0.66 T. The minimal surface roughness achieved was when using SiC powder without using a magnetic field [15]. In [16], authors studied the processes of Inconel 718 by introducing multi walled carbon nano-tubes to distilled water as an insulating fluid. It was discovered that the peak current, powder concentration, and pulse on time have significant effects on the responses; it was found that an ideal range of *MRR* and *TWR*, as well as less *SR*, could be achieved by combining Peak Current 17–20 A with Pulse on Time 270–350 µs and 1.50–2.25 g/l of multi walled carbon nano tubes concentration. Furthermore, other hard to machine materials were processed using different added powders; [17] studied the PMEDM process by adding molybdenum (Mo) powder to the insulating fluid to machine AISI H13 tool steel. The results indicated that the mechanical properties of the machined surface were improved and the fold hardness increased four times. V. T. Le studied the micro hardness and surface roughness of the SKD61 workpiece by adding tungsten carbide powder to the hydrocarbon dielectric fluid. Evaluation and analysis indicate that the addition of the powder features a beneficial influence on the characteristics of the workpiece at short pulse on time and low current. The surface roughness and micro hardness were enhanced by 53.25 % and 81.5 %, respectively, as compared to machining without powder addition [18]. G. Keskin et al. studied the effect of mixing nano graphite powder with kerosene to machine AA7075/ B_4C and AA7075/ B_4C + SiC composites. Current, pulse on time, and the reinforcement ratio were the machining parameters. Results showed that the optimum factors for material removal rate were found at 8 A of current, 150 µs of pulse on time, and 10 % of reinforcement ratio [19]. In [20] the authors tried to achieve the minimum thickness of the defect layer (recast layer) by adding graphite powder. Pulse on time, duty cycle, discharge current, and powder concentration were selected as input parameters to machine titanium alloy. The findings revealed that current was the most effective parameter on recast layer thickness, and the minimum measured thickness of it was at 1.5 A of applied current, 30 µs of applied pulse on time, 50 % of duty cycle, and 12 g/l of graphite powder concentration.

It was evident from the literature survey that there is a dearth of research on the subject of machining Inconel 718 with the use of SiO_2 nanoparticles in conjunction with the magnetic field assistance technique. Also, not much attention has been paid to studying the zone impacted by heat (*HAZ*) and the thickness of the recast layer (*WLT*) of the Inconel 718 machined surface. Therefore, within the current research, improvement of NPMEDM performance was investigated using a magnetic field assistance technique, and the effect of current, pulse on time, nano SiO_2 addition, as well as magnetic fields on process performance regarding the *WLT* and *HAZ*, in addition to the material removal rate (*MRR*), tool wear rate (*TWR*), surface roughness (*Ra*), and surface crack density (*SCD*), were evaluated.

2 EXPERIMENTAL WORK

Inconel 718 alloy was machined using (CHMER EDM) of the model CM 323+50N electrical discharge machine. 25 × 10 × 4 mm was the dimensions of the workpiece, and the chemical composition of Inconel 718 was as shown in Tab. 1. The workpiece's ultimate tensile strength and yield stress are 965 MPa and 550 MPa, respectively; its density is 8.912 g/cc; its thermal conductivity is 11.2 W/m·K; and the melting point of the workpiece is 1260–1335 °C.

Table 1 Chemical composition of Inconel 718

Element	Wt.%
C	0.03
Si	0.29
Mn	0.30
S	0.01
Cu	0.015
Cr	18.3
Ni	53
Mo	2.9
Co	0.8
Al	0.5
Ti	1.05
Nb	4.8

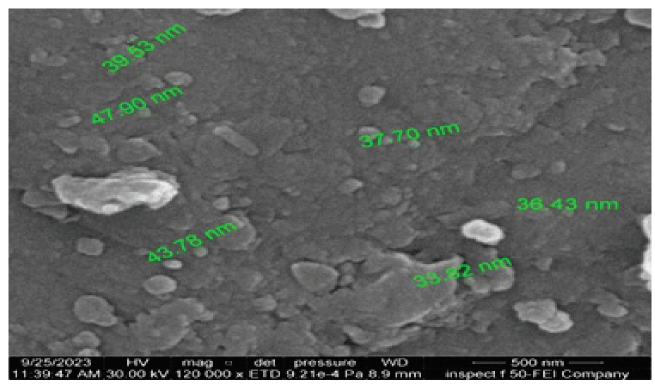

Figure 1 Nano-silicon oxide (SiO_2) particles

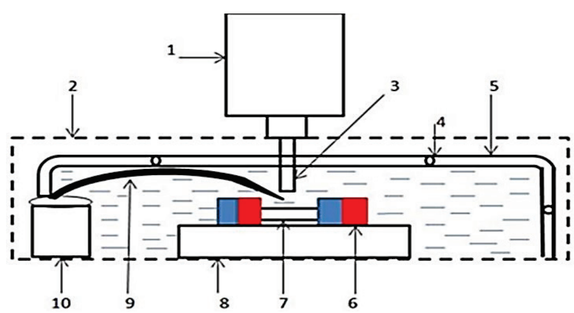

Figure 2 Scheme of MF-PMEDM: 1 – Servo system, 2 – Machining tank, 3 – Electrode, 4 – Hole, 5 – Pipe, 6 – Pair of permanent magnets, 7 – Workpiece, 8 - Vise, 9 – Flushing nozzie, 10 – Pump.

The tool electrode was made of copper; its dimensions were 15 × 10 × 70 mm. Nano-silicon oxide (SiO_2) was used as a powder additive (see Fig. 1). As an insulating fluid, soybean oil was employed in the 500 × 200 × 250 mm machining tank. Fig. 2 displays the schematic of the process, and it can be seen that the insulating fluid is flushed into the machining zone via the attached nozzle. A surfactant known as Tween60 was added to the dielectric to help keep the added nano SiO_2 suspended in the dielectric and not settle at the bottom of the tank. A magnetic field of (0.2 T) intensity was generated by a pair of permanent magnets; its intensity was examined using a digital gaussmeter device. The machining tank provided with a specific circulation system included a flushing nozzle, a pump, and a five millimeter diameter pipe that was attached within the processing tank's inside walls, this pipe was drilled with one millimeter diameter holes along its length in order to circulate the insulating fluid and avoid powder particles from collecting in the machining tank base (see Fig. 3).

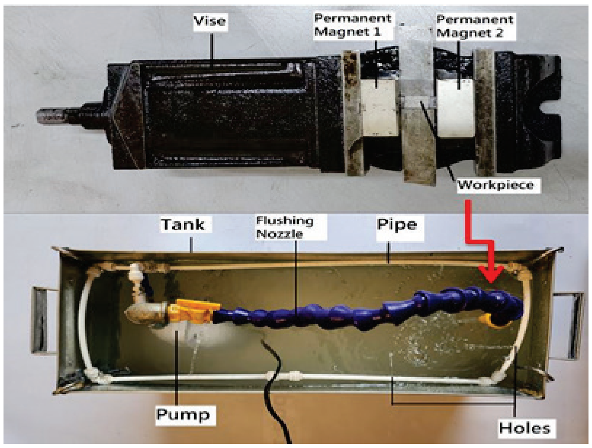

Figure 3 Machining tank

2.1 Selection of Process Parameters

Multi-level general full factorial design was used to design the experiments by Minitab 2022. The evaluated variable parameters were current (*I*), pulse on time (*Ton*), Nano SiO_2 concentration, magnetic field (*MF*) as shown in Tab. 2. The responses were white layer thickness (*WLT*), heat affected zone (*HAZ*), surface roughness (*Ra*), material removal rate (*MRR*), tool wear rate (*TWR*), and surface crack density (*SCD*). The fixed parameters were listed in Tab. 3.

Table 2 Input variables parameters

Parameter	Level 1	Level 2	Level 3
I	8 A	16 A	/
Ton	100 µs	200 µs	/
Con.	0 g/l	2 g/l	4 g/l
MF	0 T	0.2 T	/

Table 3 Fixed parameters

Parameter	Values
Pulse off time (Toff)	75 µs
Powder	SiO_2
Polarity	Straight
Gap voltage	240 V
Surfactant type	Tween60
Surfactant con.	1 ml/l
Depth of cut	1 mm

2.2 Evaluation of Experimental Outputs

An Italian OPTICA MET serial optical microscope (with high resolution optics, precise X-Y movement controls, and 10× to 100× magnification) was employed to measure the thicknesses of the recast layer and the zone impacted by heat.

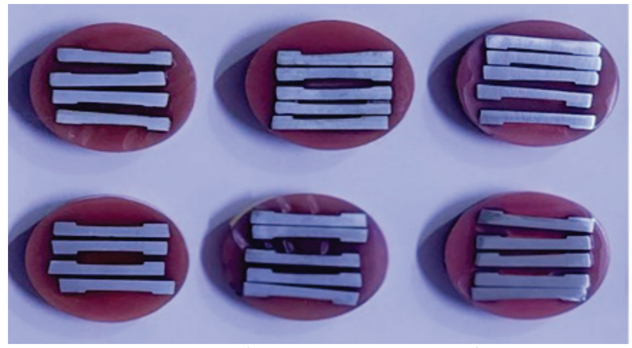

Figure 4 Prepared workpieces for measuring the thickness of white layer and heat affected zone

Prior to determining the thickness, the machined workpieces were prepared as shown in Fig. 4. The workpieces were set up in a suitable mold for grinding and polishing processes; emery paper with grit sizes of 100, 500, 1000, 1200, and 2000 was used for grinding; and polishing paper with alumina powder was used for the polishing process, followed by the etching process; then the average thicknesses of *WL* and *HAZ* were computed using the 400× magnification of the optical microscope.

Average of three readings for surface roughness was evaluated for all specimens by the Maher Fedral pocket Surf-PS1 device (the cutoff l_c was 0.25 mm automatic, the traversing length L_t was 1.75 mm automatic, and the number *n* of sampling lengths was 5).

Eq. (1) was used to calculate *MRR*, which is the specimen's weight difference before and after machining divided by the machining time and the density of Inconel 718 (0.00822 g/mm^3).

$$MRR = \frac{(W_a - W_b)}{\rho \cdot t}. \tag{1}$$

Where: W_b - the workpiece's weight in grams prior to machining; W_a - the workpiece's weight in grams following machining; ρ - the density of the Inconel 718 (0.00822 g/mm^3); t - machining time (min).

Electrode wear rate (*EWR*) which is the electrode weight that differs between electrode tool before and after machining relative to the machining time and copper density (0.008906 g/mm^3), it can be calculated as in Eq. (2).

$$EWR = \frac{(Ewt._b - Ewt._a)}{\rho \cdot t}. \tag{2}$$

Where: $Ewt._b$ - the weight of the electrode before machining (g); $Ewt._a$ - the weight of the electrode after machining (g); ρ - the density of the copper (0.008906 g/mm^3); t - machining time (min).

SCD was computed by dividing the average microcracks lengths by the micrograph's area that was captured by Axia Chemi SEM thermo scientific equipment (with thermionic tungsten filament source, automated sample navigation, a backscatter detector, and live quantitative elemental mapping), as shown in Eq. (3).

$$SCD = \frac{C_L}{A}. \tag{3}$$

Where: C_L - crack's length µm (average); A - micrograph's area (µm^2).

3 RESULTS AND DISCUSSION

3.1 Influencing Factors on White Layer Thickness (*WLT*) and Heat Affected Zone (*HAZ*)

The hardness of the machined surface is affected by *WLT*; therefore, it is essential to evaluate the effect of machining parameters on it. The *WL* develops as a consequence of the re-solidification of a portion of the melted material in the machining gap as it cools with dielectric fluid through the flushing process [21]. Since the EDM process is a thermal process, the extremely high temperature that is generated during the process alters the subsurface region structure down to a certain depth, termed the heat affected zone (*HAZ*) [22].

Adding SiO_2 nanoparticles to soybean oil result in reducing *WLT* due to the uniform distribution of energy on the machined surface; and the *WLT* was lowered due to the existence of nano SiO_2 in the machining zone, which in turn made the flushing technique more effective by enlarging the distance between the tool and the specimen and eliminating the re-solidification of debris on the machined surface. Applying greater values of pulse on time and current causes more metal to melt due to the plasma channel's raised discharge energy; therefore, more debris re-solidified and thicker *WL* produced. *MF* caused a slight rise in *WLT* when applied with the highest current value, i.e., 16 A, as shown in Fig. 5.

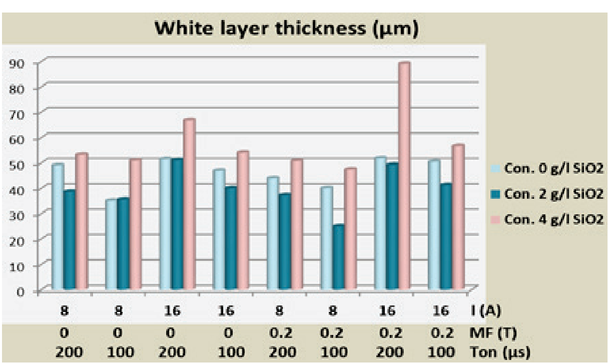

Figure 5 Effect of machining parameters on WLT of SiO_2 addition

Experimental results showed that the minimum measured *WLT* was 24.99 µm, when applying the machining conditions of run 14 (see Tab. 4). Microscopically pictures of machined specimens shown in Fig. 6. According to Tab. 5, which represents the ANOVA for *WLT*; it is noticeable that the model is statistically significant, and the more efficient parameter was current; next comes SiO_2 nanoparticles concentration and *Ton*; the effect of *MF* was insignificant.

Table 4 Results of measured *WLT*, *HAZ*, *MRR*, and *TWR*

I, A	*Ton*, µs	*Con.*, g/l	*MF*, T	*WLT*, µm	*HAZ*, µm	*Ra*, µm	*MRR*, m^3/min	*TWR*, mm^3/min
16	200	0	0.2	49.12	93.34	4.457	9.033	0.0298
8	200	2	0.2	35.2	94.557	4.413	3.619	0.0117
16	100	4	0.2	51.51	111.8	4.737	9.745	0.1684
8	100	4	0	47.02	103.02	4.304	3.266	0.0150
8	200	4	0	43.92	137.5	4.754	3.789	0.0241
8	200	0	0	40.1	92.49	4.569	3.766	0.1276
8	100	0	0	51.84	115.2	5.297	3.018	0.0983
16	100	0	0.2	50.5	73.33	4.828	8.839	0.4685
16	100	2	0.2	38.66	108	5.594	9.582	0.1567
8	100	4	0.2	35.66	74.99	5.32	3.043	0.0172
8	200	0	0.2	51.12	74.02	5.945	3.282	0.1226
16	200	4	0	40.1	132	5.852	12.11	0.1277
8	200	2	0	37.25	154.9	4.843	3.420	0.0159
8	100	2	0	24.99	53.5	4.634	3.122	0.0135
16	200	0	0	49.33	103.25	5.246	11.04	0.2824
16	200	2	0.2	41.32	107.49	5.137	10.50	0.0592
16	100	2	0	53.33	177.78	4.447	9.789	0.1402
8	200	4	0.2	50.98	86.66	4.23	3.602	0.0189
8	100	0	0.2	66.92	276.15	4.513	3.030	0.1060
16	200	4	0.2	54.17	138.35	4.347	13.63	0.0989
16	200	2	0	50.83	179.17	4.416	12.08	0.0996
8	100	2	0.2	47.49	207.83	4.469	3.835	0.0182
16	100	4	0	89.16	153.33	4.789	10.58	0.1321
16	100	0	0	56.66	140.57	4.63	10.40	0.4205

Table 5 ANOVA for WLT of SiO_2 nanoparticles addition

Source	DF	Adj SS	Adj MS	F-Value	P-Value
Model	4	2813.2	703.29	19.71	0.000
Linear	4	2813.2	703.29	19.71	0.000
I	1	841.5	841.55	23.58	0.000
Ton	1	493.3	493.35	13.83	0.001
Con.	2	1478.3	739.13	20.71	0.000
Error	19	678.0	35.68		
Total	23	3491.1			

3.2 Influencing Factors on Surface Roughness (*Ra*)

In NPMEDM, the discharge gap widens because of the existence of the added nanoparticles in the insulating medium, which disperse the discharge over the machined workpiece. In addition, the presence of these powder particles contributes to lowering the energy of the discharge, which enhances the surface quality by enabling more effective and regulated localized heat delivery [23]. Better surface finish was obtained when adding nano particles of SiO_2 to soybean oil due to the improvement in the flushing mode as a result of nanoparticles existence in the dielectric fluid which enlarge the machining gap distance. Experimental results observed that adding 2 g/l of SiO_2 causes a rise in Ra in comparison with machining without adding SiO_2 nanoparticles; while adding it with 4 g/l powder concentration led to improve the *Ra* and reduce it to values less than the values of machining without powder addition because the process became more stable, as shown in Fig. 7.

Moreover, increasing in applied current and pulse on time cause increasing in surface roughness. The minimum obtained *Ra* was 4.23 µm when applying current with 8 A, *Ton* 100 µs, 4g/l SiO_2 concentration, and without employing MF assistance, as shown in Tab. 4. The maximum measured *Ra* was 5.9447 µm when 2 g/l of SiO_2 was added, at 16 A applied current, 200 µs applied *Ton*, and without using MF, this measured value reduced to 4.5127 µm when adding the nanopowder with 4 g/l and fixing other parameters. The specimens that were machined when nano SiO_2 was added at 2 g/l and without applying MF showed a large increment in surface roughness as compared to machining without powder addition, as shown in the first four groups of columns compared to the second four groups in Fig. 7. While the surface roughness reduced slightly but was still higher than machining without powder addition when adding nano SiO_2 at 2 g/l and applying 0.2 T of magnetic field due to the effect of the magnetic field on the movement of powder particles, which contributes to regulating their movement.

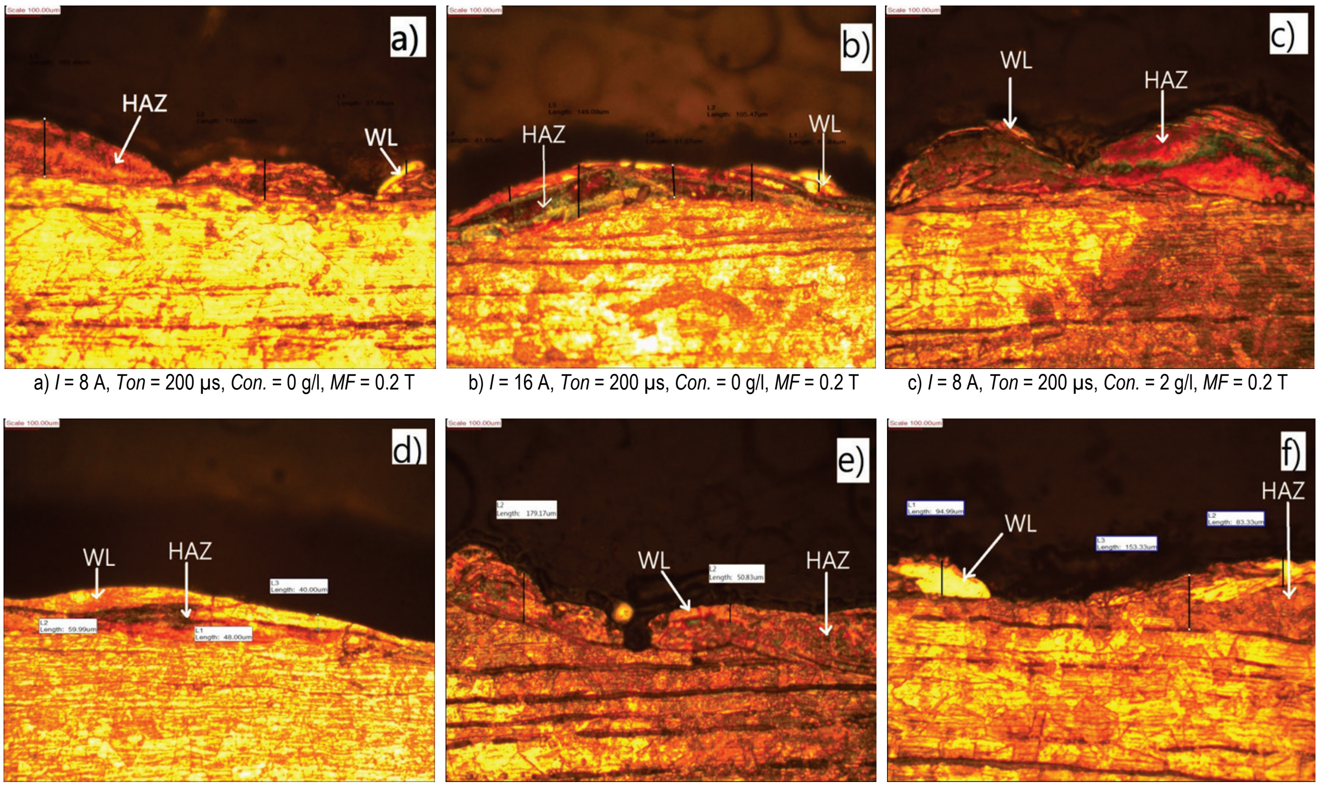

a) *I* = 8 A, *Ton* = 200 µs, *Con.* = 0 g/l, *MF* = 0.2 T
b) *I* = 16 A, *Ton* = 200 µs, *Con.* = 0 g/l, *MF* = 0.2 T
c) *I* = 8 A, *Ton* = 200 µs, *Con.* = 2 g/l, *MF* = 0.2 T
d) *I* = 16 A, *Ton* = 200 µs, *Con.* = 2 g/l, *MF* = 0.2 T
e) *I* = 8 A, *Ton* = 200 µs, *Con.* = 4 g/l, *MF* = 0.2 T
f) *I* = 16 A, *Ton* = 200 µs, *Con.* = 4 g/l, *MF* = 0.2 T

Figure 6 Microscopically pictures of WLT and HAZ

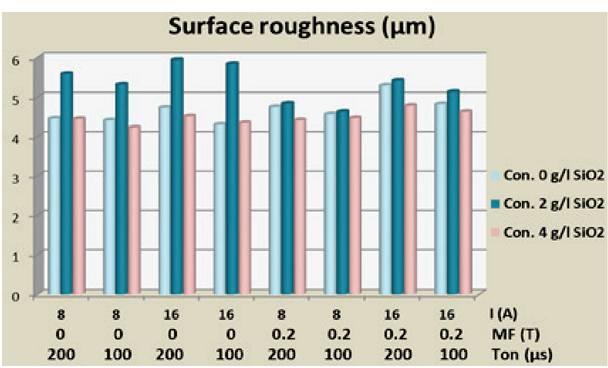

Figure 7 Machining parameter effect on *Ra* of SiO_2 nanoparticles addition

Table 6 ANOVA for Ra of SiO_2 nanoparticles addition

Source	DF	Adj SS	Adj MS	F-Value	P-Value
Model	3	3.5871	1.19570	12.57	0.000
Linear	3	3.5871	1.19570	12.57	0.000
I	1	0.4243	0.42429	4.46	0.047
Con.	2	3.1628	1.58141	16.63	0.000
Error	20	1.9021	0.09511		
Total	23	5.4892			

According to ANOVA table it appears that the concentration was the most effective parameter of *Ra* followed by current effect, and the effect of other parameters were limited (see Tab. 6).

3.3 Influencing Factors on Material Removal Rate (*MRR*)

MRR is a remarkable technical indicator in the production process of products. Production efficiency in powder mixed electrical discharge machining is dependent on the quantity of material removal per unit time. Higher *MRR*, i.e., higher production efficiency [24].

When current reaches its maximum value, the current density rises and produces a lot of thermal energy in the machining gap, which raises the *MRR*. Also, an increase in pulse on time can be attributed to the increased amount of heat generated in the machining zone, which causes the *MRR* to increase these outcomes were found to be in agreement with the study of [25]. Current is the most effective parameter on *MRR*; it is directly correlated to *MRR*, as was confirmed in the experimental results of this study. When current increases from 8A to 16A, the discharge energy increases, which leads to the melting and evaporation of the machined material, as shown in Fig. 8. The addition of nano SiO_2 to soybean oil dielectric improved *MRR*; the presence of nano particles raised the dielectric's thermal conductivity; and the frequency of the sparks increased consequently enhancing the *MRR*. When the concentration of nano SiO_2 increases from 2 g/l to 4 g/l, *MRR* increases. The minimum measured *MRR* was 3.0184 mm^3/min when applying the machining conditions without adding nanoparticles, at 8 A of applied current, 100 µs of pulse on time, and without using a magnetic field, while when adding 2 g/l of nano SiO_2, the *MRR* increased to 3.1218 mm^3/min, and when adding 4 g/l of SiO_2, it was increased to 3.2665 mm^3/min, after fixing other process parameters. The maximum obtained *MRR* was 13.6326 mm^3/min; at 16A applied current, 200 µs applied pulse on time, 4 g/l nano SiO_2 concentration, and 0.2T of MF intensity, as listed in Table 4.

From the analysis of variance (ANOVA) for *MRR* listed in Tab. 7, it can be seen that the model is statistically significant, whereas *P* values are less than 0.05. Current was the most effective parameter on *MRR*.

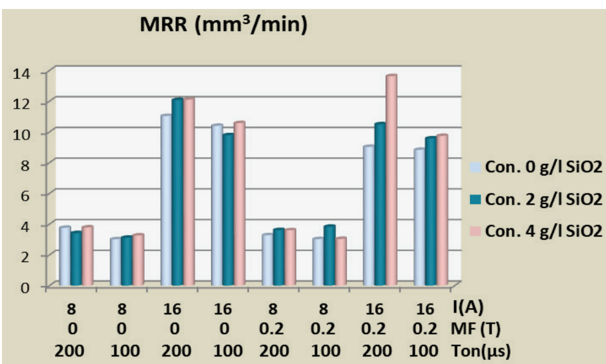

Figure 8 Effect of input parameters on *MRR*

Table 7 Analysis of variance for *MRR*

Source	DF	Adj SS	Adj MS	F-Value	P-Value
Model	7	325.756	46.537	80.77	0.000
Linear	4	321.028	80.257	139.29	0.000
I	1	312.016	312.016	541.52	0.000
Ton	1	5.627	5.627	9.77	0.007
Con.	2	3.384	1.692	2.94	0.082
2-Way Interactions	3	4.728	1.576	2.74	0.078
I×Ton	1	2.217	2.217	3.85	0.067
I×Con.	2	2.511	1.256	2.18	0.146
Error	16	9.219	0.576		
Total	23	334.975			

3.4 Influencing Factors on Tool Wear Rate (*TWR*)

TWR represents the amount of eroded material from the used tool electrode. It can be calculated by dividing the lost weight of the electrode before and after machining by the machining time multiplied by the density of the electrode material. The accuracy of the machine part is largely affected by *TWR* because the machined part is an exact copy of the electrode profile. *TWR* is affected by tool shape, tool material, melting point, current, and pulse on time [26].

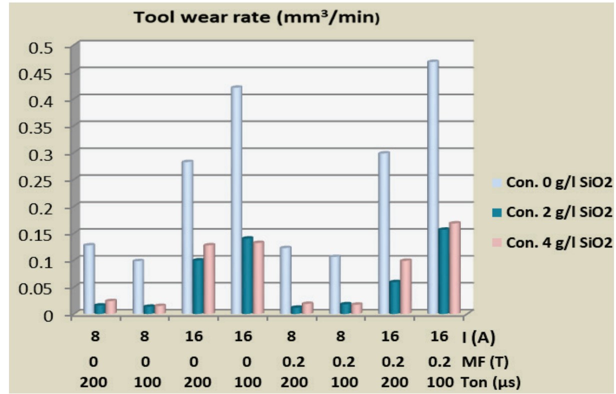

Figure 9 Effect of input parameters on TWR

As compared to the lowest obtained value for measured *TWR* in [27], which is 0.244 mm^3/min at 40 A of applied current and 400 µs of applied pulse on time to machine Inconel 718, the present study achieved lower values for measured *TWR*. The effect of machining parameters on *TWR* is shown in Fig. 9. Whereas increasing current from 8 A to 16 A caused an increase in *TWR* because of the greater discharging that generated more heat in the machining gab, which in turn led the machined metal to melt and evaporate. When *Ton* increased from 100 µs to 200 µs, it led to a slight reduction in *TWR*. This could be explained by the longer pulse on time leading to more metal to melt from the workpiece and more molten material to solidify on the surface of the electrode; thus, the MRR rises and the *TWR* reduces. Nanoparticles of SiO_2 added to soybean oil dielectric have greatly improved *TWR* through stabilizing the process by enlarging the machining gab distance between the tool and the specimen and enhancing the flashing mode, thus reducing *TWR*. On the other hand, MF has no impact on the *TWR*.

Table 8 Analysis of variance for *TWR*

Source	DF	Adj SS	Adj MS	F-Value	P-Value
Model	5	0.25884	0.051768	11.39	0.000
Linear	4	0.22935	0.057338	12.62	0.000
I	1	0.10599	0.105991	23.33	0.000
Ton	1	0.02260	0.022596	4.97	0.039
Con.	2	0.10077	0.050383	11.09	0.001
2-Way Interactions	1	0.02949	0.029489	6.49	0.020
I×Ton	1	0.02949	0.029489	6.49	0.020
Error	18	0.08178	0.004543		
Total	23	0.34062			

The minimum value for *TWR* obtained was 0.01174 mm^3/min at 8 A applied current, 200 µs applied *Ton*, 2 g/l SiO_2 nanoparticles, and 0.2 T MF intensity. The maximum measured *TWR* was 0.4685 mm^3/min without powder addition at 16 A applied current, 100 µs applied *Ton*, and 0.2 T MF, while this measured value reduced to 0.1684 mm^3/min when adding 4 g/l of nano SiO_2 and decreased to 0.156676 mm^3/min when adding 2 g/l SiO_2 nanoparticles and fixing other parameters that demonstrate the effect of powder addition to the dielectric (see Tab. 4). ANOVA of the experimental results demonstrated that current has the greatest impact on *TWR*, thereafter powder concentration and *Ton*. The impact of MF was very insignificant on *TWR* compared to other parameters. Tab. 8 represents the ANOVA for *TWR*; the model is statistically significant whereas P-values are less than 0.05.

3.5 Surface Crack Density (*SCD*)

In NPMEDM, temperature rises beyond the material's melting point to melt and evaporate the machined material; simultaneously, a rapid cooling happens, resulting in thermal stress that is higher than the machined material's fracture strength and leads to crack formation. Cracking is among the more important surface flaws that reduce the corrosion and fatigue resistance of the material [28]. Due to increases in discharge energy, microcracks generates at greater current and pulse on time applied values, which leads to an increase in thermal tendency within the solidified layer and generates more residual stresses, thus increasing the *SCD* [29]. Powder adding to the dielectric technique was used to reduce the *SCD*. When nano SiO_2 was added, a greater number of sparks were produced in the gap, the energy of the discharge was reduced, and the plasma channel became larger, resulting in fewer cracks. The machined surface was seen to have complicated looks through the SEM micrograph, which included spherical particles, craters, voids, and cracks. As shown in Fig. 10a, the surface machined by adding nano SiO_2 has fewer cracks as compared to Fig. 10b, which was processed with no adding nano SiO_2 at the same magnification. To compute the amount of cracking, the *SCD* measures the average cracks' length per unit area. *SCD* for specimen machined at 16 A applied current, 200 µs applied *Ton*, 0.2 T *MF* intensity, and adding 4 g/l nano SiO_2 was 0.00313 µm/µm^2, and the *SCD* of specimen machined with the same applied conditions but without the addition of nano SiO_2 was 0.00359 µm/µm^2.

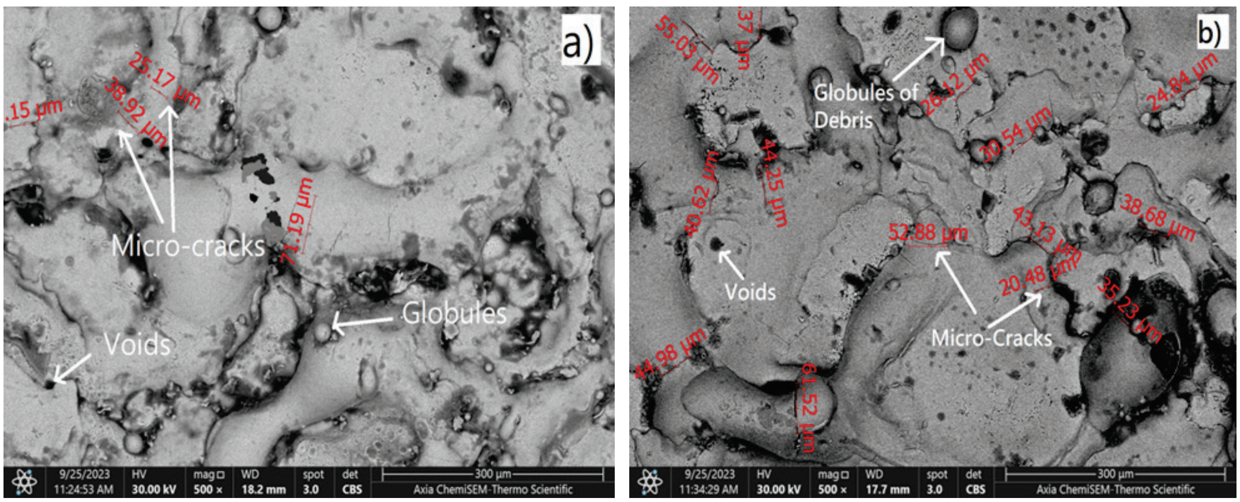

Figure 10 Cracks of machined surface with *I* = 16 A, *Ton* = 200µs, *MF* = 0.2 T, and (a) 4 g/l of nano SiO_2, (b) without adding powder.

4 CONCLUSIONS

For the purpose of enhancing its performance, the NPMEDM was examined in the current study. Nanoparticles of SiO_2 were introduced to soybean oil, a fluid employed as insulation. Practical experiments were concluded to evaluate the influence of controlling factors, in the context of peak current, pulse on time, SiO_2 nanoparticle concentration, and magnetic field, on NPMEDM performance with respect to *WLT*, *HAZ*, *Ra*, *MRR*, *TWR*, and *SCD*.

The outcomes of the experiments demonstrated that the addition of SiO_2 nanoparticles to the insulating fluid led to improved process's performance with regard of all the outputs (*WLT*, *HAZ*, *Ra*, *MRR*, *TWR*, and *SCD*). The minimum *WLT* and *HAZ* were 24.99 and 53.5 µm, respectively, when applying the machining conditions of 8A of applied current, 100 µs of applied *Ton*, and 2 g/l of SiO_2 nanoparticles without using *MF*. The lowest amount attained of *Ra* was 4.23 µm when applying 8 A of current, 100 µs of *Ton*, 4 g/l of SiO_2 concentration, and without employing *MF*. The maximum obtained *MRR* was 13.6326 mm^3/min at 16 A applied current, 200 µs applied pulse on time, 4 g/l nano SiO_2 concentration, and applying 0.2 T of *MF* intensity. The minimum value for *TWR* obtained was 0.01174 mm^3/min at 8A applied current, 200 µs applied *Ton*, 2 g/l SiO_2 nanoparticles concentration, and 0.2 T *MF* intensity. Lower *SCD* was obtained when adding 4 g/l of SiO_2 nanoparticles to the used insulating fluid; it was 0.00313 µm/µm^2, while the *SCD* was 0.00359 µm/µm^2 when machining without adding SiO_2 nanoparticles to the insulating fluid. Run #14 has the optimal combination of applied process parameters (current of 8 A applied value, pulse on time of 100 µs, nano SiO_2 of 2 g/l, and 0.2 T of magnetic field intensity).

NPMEDM is a crucial step in the machining of superalloys, though its mechanisms are still poorly understood, and this study aims to improve the process performance. Subsequent research efforts could delve deeper into the underlying mechanism. To fully understand how the type of the nanoparticle, its shape, and its size affect the machined part's corrosion resistance, fatigue, and surface integrity, more research is required. Further, investigations might be looking into optimization of nanoparticles parameters to improve the effectiveness and reliability of the NPMEDM. Future research can yield insightful information by addressing these factors, and this could help in the development of more efficient machining for advanced materials.

5 REFERENCES

[1] Mookam, N., Sunasuan, P., Madsa, T., Muangnoy, P. & Chuvaree, S. (2021). Effects of Graphite and Boron Carbide Powders Mixed into Dielectric Fluid on Electrical Discharge Machining of SKD 11 Tool Steel. *Arab. J. Sci. Eng.*, 46(3), 2553-2563. https://doi.org/10.1007/s13369-020-05156-4

[2] Payal, H., Bharti, P. S., Maheshwari, S. & Agarwal, D. (2020). Machining characteristics and parametric optimisation of inconel 825 during electric discharge machining. *Teh. Vjesn., 27*(3), 761-772. https://doi.org/10.17559/TV-20190214135509

[3] Ibrahim, A. F. (2022). Evaluation of Surface Roughness And Material Removal Rate in Electrical Discharge Machining of Al-Alloy With 10% SiC. *IIUM Eng. J., 23*(1), 349-357. https://doi.org/10.31436/IIUMEJ.V23I1.2114

[4] Shirguppikar, S. et al. (2021). Assessing the effects of uncoated and coated electrode on response variables in electrical discharge machining for ti-6al-4v titanium alloy. *Tribol. Ind., 43*(4), 524-534. https://doi.org/10.24874/ti.1020.12.20.03

[5] Singh, R. K., Tiwari, S. K., Srivastava, S. C. & Kumar, B. (2023). Hybrid Taguchi-GRA-CRITIC Optimization Method for Multi-Response Optimization of Micro-EDM Drilling Process Parameters. *Teh. Vjesn., 30*(3), 804-814. https://doi.org/10.17559/TV-20220601114015

[6] Nguyen, T. T. & Nguyen, K. D. (2021). Multi-attribute optimization of the wedm process for surface characteristics and productivity. *Teh. Vjesn., 28*(2), 473-480. https://doi.org/10.17559/TV-20190728094458

[7] Gul, I. A., Abdul-Rani, A. M., Al-Amin, M. & Garba, E. (2023). Elucidating Powder-Mixed Electric Discharge Machining Process, Applicability, Trends and Futuristic Perspectives. *Machines, 11*(3). https://doi.org/10.3390/machines11030381

[8] Kavade, M. V., Mohite, S. S. & Unaune, D. R. (2019). Application of metal powder to improve metal removal rate in Electric Discharge Machining. *Mater. Today Proc*., 16, 398-404. https://doi.org/10.1016/j.matpr.2019.05.107

[9] Ahmad, S. et al. (2017). Powder Mixed Dielectric in Electrical Discharge Machining of Inconel 718. *J. Mech. Eng., SI 4*(3), 110-127.

[10] Jadam, T., Sahu, S. K., Datta, S. & Masanta, M. (2019). EDM performance of Inconel 718 superalloy: application of multi-walled carbon nanotube (MWCNT) added dielectric media. *J. Brazilian Soc. Mech. Sci. Eng., 41*(8). https://doi.org/10.1007/s40430-019-1813-9

[11] Paswan, K., Pramanik, A. & Chattopadhyaya, S. (2020). Machining performance of Inconel 718 using graphene nanofluid in EDM. *Mater. Manuf. Process., 35*(1), 33-42. https://doi.org/10.1080/10426914.2020.1711924

[12] Ranjan, A., Chakraborty, S., Kumar, D. & Bose, D. (2020). An Investigation on Surfactant Added PMWEDM of Inconel 718. *Int. J. Automot. Mech. Eng., 17*(3), 8140-8149. https://doi.org/10.15282/ijame.17.3.2020.07.0611

[13] Elumalai, B., Gowri, S., Hariharan, P. & Arun Pillai, K. V. (2022). Experimental investigations on μeD milling of inconel 718 with nano SiC abrasive mixed dielectric. *Mater. Res., 25*. https://doi.org/10.1590/1980-5373-MR-2021-0468

[14] R. K. Patel and M. K. Pradhan, (2023). Machining of nickel-based super alloy inconel 718 using alumina nanofluid in powder mixed electric discharge machining. *Mater. Res. Express, 10*(3). https://doi.org/10.1088/2053-1591/acbae8

[15] Kumar, S., Goud, M. & Suri, N. M. (2021). An Investigation of Magnetic-field-assisted EDM by Silicon and Boron Based Dielectric of Inconel 706. *Silicon, 13*, 4747-4755. https://doi.org/10.1007/s12633-020-00776-9

[16] Khatun, S., Amin, A. K. M. N., Mashuk, M. R., Tuli, N. T., Jerin, I., Bashar, M. S. & Rumi Md, J. U. (2024). Parameter optimization and surface integrity aspects in MWCNT-based nano-PMEDM process of Inconel 718. *Res. Eng. Struct. Mater., 10*(1), 271-304. https://doi.org/10.17515/resm2023.18ma0530rs

[17] Amorim, F. L., Dalcin, V. A., Soares, P. & Mendes, L. A. (2017). Surface modification of tool steel by electrical discharge machining with molybdenum powder mixed in dielectric fluid. *Int. J. Adv. Manuf. Technol.*, *91*(1-4), 341-350. https://doi.org/10.1007/s00170-016-9678-x

[18] Le, V. T. (2021). The role of electrical parameters in adding powder influences the surface properties of SKD61 steel in EDM process. *J. Brazilian Soc. Mech. Sci. Eng., 43*(3), 1-19. https://doi.org/10.1007/s40430-021-02844-6

[19] Keskin, G., Salunkhe, S., Küçüktürk, G., Pul, M., Gürün, H. & Baydaroğlu, V. (2023). Optimization of PMEDM process parameters for B4C and B4C+SiC reinforced AA7075 composites. *J. Eng. Res.* https://doi.org/10.1016/j.jer.2023.09.012

[20] Rodic, D., Gostimirovic, M., Sekulic, M., Savkovic, B. & Aleksic, A. (2023). Study and Optimization Defect Layer in Powder Mixed Electrical Discharge Machining of Titanium Alloy. *Processes, 11*(4). https://doi.org/10.3390/pr11041289

[21] Muthuramalingam, T. & Phan, N. H. (2021). Experimental Investigation of White Layer Formation on Machining Silicon Steel in PMEDM Process. *Silicon, 13*, 2257-2263. https://doi.org/10.1007/s12633-020-00740-7

[22] Talla, G., Gangopadhyay, S. & Biswas, C. K. (2023). Influence of powder-mixed EDM on surface morphology and metallurgical alterations of Inconel 625. *Aust. J. Mech. Eng., 21*(5), 1533-1546. https://doi.org/10.1080/14484846.2021.2022580

[23] Paswan, K. et al. (2023). An analysis of microstructural morphology, surface topography, surface integrity, recast layer, and machining performance of graphene nanosheets on Inconel 718 superalloy: Investigating the impact on EDM characteristics, surface characterizations, and opt. *J. Mater. Res. Technol., 27*, 7138-7158. https://doi.org/10.1016/j.jmrt.2023.11.080

[24] Ming, W. et al. (2022). Research on EDM Performance of Renewable Dielectrics under Different Electrodes for Machining SKD11. *Crystals, 12*(2). https://doi.org/10.3390/cryst12020291

[25] Khadar, B. S. Jagannadha, R. M. V. & Murahari, K. (2021). Multi-Objective Optimization of Process Parameters for Powder Mixed Electrical Discharge Machining of Inconel X-750 Alloy Using Taguchi-Topsis Approach. *Strojnícky časopis - Journal of Mechanical Engineering, 71*(1), 1-18. https://doi.org/10.2478/scjme-2021-0001

[26] Gerçekcioğlu, E. & Albaşkara, M. (2023). Multi-Response Optimization of Electrical Discharge Machining of 17-4 Ph Ss Using Taguchi-Based Grey Relational Analysis. *Arch. Metall. Mater., 68*(3), 861-868. https://doi.org/10.24425/amm.2023.145448

[27] Lajis, M. A. & Ahmad, S. (2015). Machinability performance of powder mixed dielectric in electrical discharge machining (EDM) of inconel 718 with copper electrode. *Int. J. Mech. Mechatronics Eng., 15*(4), 37-52.

[28] Reddy, V. V., Kumar, A., Valli, P. M. et al. (2015). Influence of surfactant and graphite powder concentration on electrical discharge machining of PH17-4 stainless steel. *J Braz. Soc. Mech. Sci. Eng., 37*, 641-655. https://doi.org/10.1007/s40430-014-0193-4

[29] Srivastava, S., Vishnoi, M., Gangadhar, M. T. & Kukshal, V. (2023). An insight on Powder Mixed Electric Discharge

Machining: A state of the art review. *Proc. Inst. Mech. Eng. Part B J. Eng. Manuf., 237*(5), 657-690.
https://doi.org/10.1177/09544054221111896

Authors' contacts:

Dunya Adnan Ghulam
(Corresponding author)
Production Engineering and Metallurgy Dept.,
University of Technology,
Alsina'a Street, 10066 Baghdad, Iraq
dunia.a.ghulam@gmail.com

Abbas Fadhil Ibrahim, Professor
Production Engineering and Metallurgy Dept.,
University of Technology,
Alsina'a Street, 10066 Baghdad, Iraq
abbas.f.ibrahim@uotechnology.edu.iq